A New Model for Predicting the Hydraulic Conductivity of Unsaturated Porous Media

YECHEZKEL MUALEM

Faculty of Civil Engineering, Technion-Israel Institute of Technology, Haifa, Israel

A simple analytic model is proposed which predicts the unsaturated hydraulic conductivity curves by using the moisture content–capillary head curve and the measured value of the hydraulic conductivity at saturation. It is similar to the Childs and Collis-George (1950) model but uses a modified assumption concerning the hydraulic conductivity of the pore sequence in order to take into account the effect of the larger pore section. A computational method is derived for the determination of the residual water content and for the extrapolation of the water content–capillary head curve as measured in a limited range. The proposed model is compared with the existing practical models of Averjanov (1950), Wyllie and Gardner (1958), and Millington and Quirk (1961) on the basis of the measured data of 45 soils. It seems that the new model is in better agreement with observations.

INTRODUCTION

The various models used for predicting the hydraulic conductivity of unsaturated soils were reviewed by *Brutsaert* [1967]. We may distinguish between two main groups. The first is based on a generalization of Kozeny's approach for saturated and unsaturated porous media, according to which the relative hydraulic conductivity K_r is a power function of the effective saturation S_e, i.e.,

$$K_r = K/K_{sat} = S_e^{\alpha} \tag{1}$$

where

$$S_e = (\Theta - \Theta_r)/(\Theta_{sat} - \Theta_r) \tag{2}$$

where Θ and Θ_r are the actual and the residual water content, respectively. Following this approach, *Averjanov* [1950] proposed the value $\alpha = 3.5$, whereas *Irmay* [1954] derived (1) theoretically with $\alpha = 3.0$. It seems that for a wide variety of soils, $\alpha = 3.5$ leads to a better agreement with observations [*Brooks and Corey*, 1964; *Boreli and Vachaud*, 1966].

The second group includes the models of *Burdine* [1953], *Wyllie and Gardner* [1958] (WG in this paper), *Farrell and Larson* [1972], and *Childs and Collis-George* [1950] (CCG in this paper) and the modifications to the CCG model proposed by *Marshall* [1958], *Millington and Quirk* [1961] (MQ in this paper), and *Kunze et al.* [1968]. The models of this group make use of the measured capillary head–water content $\psi(\Theta)$ curve to derive the hydraulic conductivity in the unsaturated state. While in petroleum engineering the 'Burdine equation'

$$K_r(\theta) = S_e^2 \int_{\theta=0}^{\theta} d\theta/\psi^2 \Big/ \int_{\theta=0}^{\theta_{sat}} d\theta/\psi^2 \tag{3}$$

$$\theta = \Theta - \Theta_r$$

is commonly used, soil scientists refer generally to a modified form of the CCG equation,

$$K_r(\theta_l) = S_e^{\beta} \sum_{i=1}^{l} \frac{[2(l-i)+1]}{\psi_i^2} \Big/ \sum_{i=1}^{m} \frac{[2(m-i)+1]}{\psi_i^2} \tag{4}$$

Here m represents the total number of intervals into which the θ domain is divided, and l is the number of intervals up to a prescribed value of θ. CCG, MQ, and Kunze et al. suggest $\beta =$ 0, ½, and 1, respectively. *Jackson et al.* [1965], *Kunze et al.* [1968], *Green and Corey* [1971], and *Bruce* [1972] have checked the reliability of (4). It seems that the MQ formula is in somewhat better agreement with measured data than the other formulae.

The three main models represented by (1), (3), and (4) do not seem to have been tested together against measured data before.

The purpose of the present study is to propose a new simplified model which minimizes the deviations between predicted and measured $K(\Theta)$ curves.

THEORY

We consider a homogeneous porous medium, having interconnected pores defined by their radius r. The contribution of full pores of radii $r \to r + dr$ to θ is

$$f(r)\,dr = d\theta \tag{5}$$

where $f(r)$ is the pore water distribution function. We have

$$\int_{R_{min}}^{R} f(r)\,dr = \theta(R) \tag{6}$$

and in particular,

$$\int_{R_{min}}^{R_{max}} f(r)\,dr = \theta_{sat} \tag{7}$$

The areal porosity is equal here to the volumetric porosity, so $f(r)\,dr$ represents the ratio between the pore area of radii $r \to r + dr$ and the total area. Consider a porous slab of thickness Δx ($x \to x + \Delta x$ along the axis). The pore area distribution at the two slab sides is identical. For $\Delta x \gg R_{max}$, complete randomness of the relative positions of the two slab faces is assumed. The probability of pores of radii $r \to r + dr$ at x encountering pores of radii $\rho \to \rho + d\rho$ at $x + \Delta x$ is

$$a(r, \rho) = f(r)f(\rho)\,dr\,d\rho \tag{8}$$

Here no direct connection between the pores r and ρ does exist along the x axis. The other extreme case occurs when $\Delta x \to 0$. Then the correlation between the two slab faces is complete. Since we are concerned with the effect of pore changes on the hydraulic conductivity, it is more relevant to consider Δx to be of the same order of magnitude as the pore radii. Then the probability of the connection of a pore $r \to r + dr$ to a pore $\rho \to \rho + d\rho$ is

Copyright © 1976 by the American Geophysical Union.

$$a(r, \rho) = G(R, r, \rho)f(r)f(\rho)\, dr\, d\rho \tag{9}$$

$G(R, r, \rho)$ is a correction accounting for partial correlation between the pores r and ρ at a given water content $\theta(R)$.

The contribution of the actual flow configuration in the slab to the hydraulic conductivity cannot be accurately assessed. We use, therefore, two simplifying assumptions: (1) there is no bypass flow between the slab pores, and (2) the pore configuration may be replaced by a pair of capillary elements (Figure 1) whose lengths are proportional to their radii:

$$l_1/l_2 = r/\rho \tag{10}$$

The hydraulic conductivity is then found to vary as $r\rho$ (see Appendix 1). If we use a correction factor $T(R, r, \rho) < 1$ to account for eccentricity of the flow path (tortuosity factor), the contribution of the $r \rightarrow \rho$ element to the relative conductivity becomes

$$dK_r(r, \rho) = \frac{T(R, r, \rho)G(R, r, \rho)r\rho f(r)f(\rho)\, dr\, d\rho}{\int_{R_{min}}^{R_{max}} \int_{R_{min}}^{R_{max}} T(R_{max}, r, \rho)G(R_{max}, r, \rho)r\rho f(r)f(\rho)\, dr\, d\rho} \tag{11}$$

For a given $\theta(R)$ the corresponding $K_r(\theta)$ is

$$K_r(\theta) = \frac{\int_{R_{min}}^{R} \int_{R_{min}}^{R} T(R, r, \rho)G(R, r, \rho)r\rho f(r)f(\rho)\, dr\, d\rho}{\int_{R_{min}}^{R_{max}} \int_{R_{min}}^{R_{max}} T(R, r, \rho)G(R, r, \rho)r\rho f(r)f(\rho)\, dr\, d\rho} \tag{12}$$

Since there exists no procedure for an independent determination of $T(R, r, \rho)$ and $G(R, r, \rho)$, we assume with *Burdine* [1953] and MQ that the tortuosity and correlation factors are power functions of θ, thus depending solely on R. Hence

$$K_r(\theta) = S_e^n \frac{\int_{R_{min}}^{R} rf(r)\, dr \int_{R_{min}}^{R} \rho f(\rho)\, d\rho}{\int_{R_{min}}^{R_{max}} rf(r)\, dr \int_{R_{min}}^{R_{max}} \rho f(\rho)\, d\rho} = S_e^n \left[\frac{\int_{R_{min}}^{R} rf(r)\, dr}{\int_{R_{min}}^{R_{max}} rf(r)\, dr}\right]^2 \tag{13}$$

Applying the capillary law $r = C/\psi$ and (5) to (13), one obtains

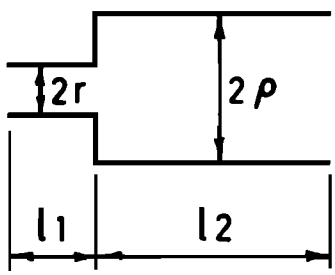

Fig. 1. A combination of cylindrical tubes used to evaluate the hydraulic conductivity of a pair of capillary elements.

$$K_r(\theta) = S_e^n \left[\int_0^{\theta} d\theta/\psi \Big/ \int_0^{\theta_{sat}} d\theta/\psi\right]^2 \tag{14}$$

where n may be positive or negative. Equation (14) is very simple and easy to apply. For $\psi(\theta)$ given in analytical form, $K_r(\theta)$ can be derived explicitly. For example, introducing in (14) the expression used by *Brooks and Corey* [1964],

$$S_e = (\psi/\psi_{cr})^{-\lambda} \tag{15}$$

yields

$$K_r(S_e) = S_e^{n+2+2/\lambda} \tag{16}$$

$$K_r(\psi) = (\psi/\psi_{cr})^{-2-\lambda(2+n)} \tag{17}$$

With $n = 0$, (16) and (17) reduce to the equations obtained by *Brutsaert* [1967], using the CCG model. However, the inclusion of n (which accounts for the correlation between pores and for the flow path tortuosity) in (16) and (17) contributes to a more flexible formula of $K_r(S_e)$ and therefore to a greater chance of agreement between theoretical and experimental curves. Another example is *Farrell and Larson*'s [1972] formula

$$\psi = \psi_{cr}e^{\alpha(1-S_e)} \tag{18}$$

which when it is substituted into (14) leads to

$$K_r(S_e) = S_e^n(e^{2\alpha S_e} - 2e^{\alpha S_e} + 1)/(e^{2\alpha} - 2e^{\alpha} + 1) \tag{19}$$

It is not clear whether (16) or (19) is in better agreement with measured data. Equation (16), however, is easier to use in the derivation of analytical solutions of complicated unsaturated flows.

COMPUTED RESULTS

Before agreement of theory with measurements and comparison with other methods can be examined, the residual water content Θ_r and the power n of S_e ((14)) must be determined. The influence of using partial and complete ψ-Θ curves on the computed hydraulic conductivity was checked by *Kunze et al.* [1968]. It seems that complete ψ-Θ information improves the quality of the prediction mainly as a result of a better fulfillment of the requirement that $K = 0$ for $\Theta = \Theta_r$. They recommend, therefore, extrapolation of the measured portion of the ψ-Θ curve. During the present study we realized that because of the strong sensitivity of the computed $K(\Theta)$ curve to the value of Θ_r, the decision about which model compares more favorably with experimental data of a given soil is, in fact, governed by Θ_r. For this reason, we think that it is necessary to use a standard analytical procedure to fix a value of Θ_r and to extrapolate a partially given ψ-Θ curve. We propose herein a convenient procedure, based on the assumption that the soil characteristic curve in the extrapolation range can be analytically represented by (15), which fulfils the condition $\psi \rightarrow \infty$ for $\Theta \rightarrow \Theta_r$. Parameters Θ_r and λ are computed with the aid of a minimum square deviation procedure for regression of measured ψ-Θ points to (15) in the range $\Theta < \Theta_p$, where Θ_p is the value at which the measured curve shows an inflection point (Appendix 2).

Now if we perform a similar fitting procedure for the $K_r(\theta)$ curve to (14), we can expect to get different values of n for different soils. As was already mentioned, the value of n may be negative too. Of course, this poses a great difficulty if one is interested in a universal $K_r(\theta)$ representation, valid for all soils. As a sort of compromise between both representations, it is suggested that an expression be adopted for which the square

deviation, averaged over a great number of soils, is minimum. In essence, n becomes an experimentally determined parameter.

Forty-five soils for which measured ψ-Θ and K-θ (or K-ψ) data on drainage are available in the literature were used for computation. In Table 1 a list of the soils, their measured Θ_{min}, ψ_{min}, and Θ_{max}, the computed Θ_r obtained by using the procedure suggested in Appendix 2, and the power λ of S_e are given. For each soil the mean square deviation D between the measured hydraulic conductivities K_{rm} and the computed ones K_{rc},

$$D = \left\{\int_{S_{e\,min}}^{1} [\ln(K_{rc}) - \ln(K_{rm})]^2 \frac{dS_e}{(1 - S_{e\,min})}\right\}^{1/2} \quad (20)$$

is computed. Eight different values of n were used (substituted in (14)): $n = -1 + 0.5j, j = 0, 1, \cdots, 7$. In order to maintain consistency in the numerical computation of D for all soils we have used a constant increment $\Delta S_e = 0.02$. In Table 2 the mean value $\bar{D}$, the standard deviation σ, and the coefficient of variance ϵ for the 45 soils are given as a function of n. The continuous graph of $\bar{D}(n)$ as plotted in Figure 2 shows that $n = 0.5$ may indeed hold as the best value. Hence the suggested formula for $K_r(S_e)$ becomes

$$K_r(S_e) = S_e^{1/2}\left(\int_0^{S_e} dS_e/\psi \Big/ \int_0^1 dS_e/\psi\right)^2 \quad (21)$$

In practice, we distinguish between the extrapolated region $0 \le S_e < S_{e\,min}$ ($\Theta_r < \Theta < \Theta_{min}$), for which an analytical expression ((15)) is used to represent the ψ-S_e curve, and the measured region $S_{e\,min} \le S_e \le 1$, where the computation is carried out numerically. Continuity requires that the extrapolated curve meet the measured one at (ψ_{min}, $S_{e\,min}$). Thus (21) becomes

$$K_r(S_e) = S_e^{1/2}\left[\frac{S_{e\,min}/(1 + 1/\lambda)\psi_{min} + \int_{S_{e\,min}}^{S_e} dS_e/\psi}{S_{e\,min}/(1 + 1/\lambda)\psi_{min} + \int_{S_{e\,min}}^{1} dS_e/\psi}\right]^2 \quad (22)$$

while the WG model ((3)) yields

TABLE 1. Computed Θ_r and λ for the 45 Soils

No.	Soil Index	References	Θ_{max}	Θ_{min}	ψ_{min}, cm H_2O	Θ_r	λ
1	1006	Beit Netofa clay [*Rawitz*, 1965]	0.446	0.241	1.51×10^4	0.010	0.19
2	1101	Shluhot silty clay [*Rawitz*, 1965]	0.385	0.163	1.51×10^4	0.010	0.20
3	2002	Silt Mont Cenis [*Vachaud*, 1966]	0.447	0.042	1.70×10^5	0.010	0.36
4	2004	Slate dust [*Childs and Collis-George*, 1950]	0.482	0.110	1.44×10^2	0.090	5.69
5	3001	Weld silty clay loam [*Jensen and Hanks*, 1967]	0.470	0.140	2.12×10^2	0.090	1.52
6	3002	Amarillo silty clay loam [*Brooks and Corey*, 1966]	0.455	0.140	2.25×10^2	0.110	2.35
7	3101	Rideau clay loam [*Topp*, 1971]	0.416	0.286	4.19×10^2	0.280	1.62
8	3301	Caribou silt loam [*Topp*, 1971]	0.441	0.313	4.25×10^2	0.280	0.91
9	3302	Grenville silt loam [*Staple*, 1965]	0.475	0.037	1.00×10^6	0.010	0.34
10	3304	Touchet silt loam [*Jensen and Hanks*, 1967]	0.480	0.170	2.35×10^2	0.120	1.71
11	3305	Ida silt loam (>15 cm) [*Green et al.*, 1964]	0.530	0.175	2.00×10^3	0.060	0.38
12	3306	Ida silt loam (0–15 cm) [*Green et al.*, 1964]	0.554	0.219	2.00×10^3	0.010	0.27
13	3307	Touchet silt loam (General Electric 3) [*Brooks and Corey* 1964]	0.469	0.180	4.14×10^2	0.130	1.89
14	3403	Pachappa loam [*Jackson et al.*, 1965]	0.456	0.007	3.19×10^6	0.002	0.42
15	3404	Adelanto loam [*Jackson et al.*, 1965]	0.426	0.012	4.65×10^6	0.007	0.50
16	3405	Indio loam [*Gardner*, 1959]	0.450	0.021	1.50×10^6	0.010	0.81
17	3407	Guelph loam [*Elrick and Bowman*, 1964]	0.520	0.236	1.00×10^3	0.130	0.41
18	3501	Rubicon sandy loam [*Topp*, 1969]	0.381	0.166	2.40×10^2	0.150	2.08
19	3503	Pachappa fine sandy clay [*Elrick and Bowman*, 1964]	0.334	0.049	1.50×10^4	0.030	0.44
20	3504	Gilat sandy loam [*Hadas*, 1967]	0.440	0.130	1.02×10^3	0.010	0.44
21	4106	Sand [*Poulovassilis*, 1970]	0.272	0.090	3.60×10^1	0.010	1.83
22	4107	Sand [*Poulovassilis*, 1970]	0.258	0.084	3.80×10^1	0.010	2.87
23	4109	Botany sand fraction (150–300 μm) [*Watson*, 1967]	0.350	0.055	5.70×10^1	0.040	8.35
24	4111	River sand (screened) [*Jensen and Hanks*, 1967]	0.400	0.060	1.50×10^2	0.050	1.57
25	4114	Volcanic sand [*Jensen and Hanks*, 1967]	0.350	0.050	1.85×10^2	0.040	1.30
26	4116	Sand fraction (150–300 μm) [*Kastelanek*, 1971]	0.372	0.045	8.00×10^1	0.040	4.94
27	4118	Sable de rivière [*Vachaud*, 1966]	0.342	0.075	1.90×10^2	0.060	0.92
28	4120	Gilat fine sand [*Rawitz*, 1965]	0.179	0.070	1.51×10^4	0.010	0.27
29	4121	Rehovot sand [*Hadas*, 1967]	0.400	0.020	2.50×10^3	0.015	0.83
30	4123	Pouder River sand [*Brooks and Corey*, 1966]	0.364	0.044	8.20×10^1	0.030	2.92
31	4126	Molonglo River sand [*Talsma*, 1970]	0.277	0.098	3.00×10^1	0.010	0.96
32	4129	Beit Dagan sand [*Rawitz*, 1965]	0.161	0.052	1.49×10^4	0.040	0.37
33	4130	Hygiene sandstone [*Brooks and Corey*, 1964]	0.250	0.151	2.01×10^2	0.140	3.78
34	4131	Berea sandstone [*Brooks and Corey*, 1964]	0.206	0.064	2.34×10^2	0.050	2.13
35	4132	Fragmented Fox Hill sandstone [*Brooks and Corey*, 1964]	0.503	0.166	1.16×10^2	0.160	2.61
36	4133	Fine sand (General Electric 13) [*Brooks and Corey*, 1964]	0.356	0.063	3.02×10^2	0.050	1.98
37	4134	Volcanic sand [*Brooks and Corey*, 1964]	0.365	0.058	2.73×10^2	0.050	1.65
38	4137	Sand fraction (150–300 μm) [*Watson*, 1967]	0.350	0.056	5.70×10^1	0.050	11.67
39	4141	Sand fraction (1.0–0.5 mm) [*Childs and Collis-George*, 1950]	0.357	0.034	3.64×10^1	0.020	2.80
40	4142	Sand fraction (0.5–0.25 mm) [*Childs and Collis-George*, 1950]	0.364	0.040	4.40×10^1	0.030	5.69
41	4143	Fragmented mixture [*Brooks and Corey*, 1964]	0.437	0.134	1.07×10^2	0.120	2.65
42	4147	Plainfield sand (25–60 cm) [*Black et al.*, 1969]	0.307	0.060	2.05×10^2	0.050	1.45
43	5002	Glass beads [*Brooks and Corey*, 1964]	0.383	0.037	3.01×10^2	0.030	1.90
44	5003	Aggregated glass beads [*Topp and Miller*, 1966]	0.548	0.080	8.26×10^1	0.060	3.57
45	5004	Monodispersed glass beads [*Topp and Miller*, 1966]	0.326	0.033	6.82×10^1	0.020	6.24

Θ_{max}, Θ_{min}, and Θ_r are given in percent of total volume.

TABLE 2. Computed $\bar{D}$, σ, and ϵ for Eight Values of n Obtained by Using (14)

	n							
	−1.0	−0.5	0.0	0.5	1.0	1.5	2.0	2.5
$\bar{D} = \sum D_i/45$	1.40	1.18	1.01	0.97	1.09	1.32	1.62	1.94
$\sigma = [(D_i - \bar{D})^2/45]^{1/2}$	0.73	0.70	0.75	0.82	0.89	0.96	1.04	1.58
$\epsilon = \sigma/\bar{D}$	0.52	0.60	0.74	0.84	0.81	0.72	0.64	1.13

$$K_r(S_e) = S_e^2 \frac{S_{e\min}/(1 + 2/\lambda)\psi_{\min}^2 + \int_{S_{e\min}}^{S_e} dS_e/\psi^2}{S_{e\min}/(1 + 2/\lambda)\psi_{\min}^2 + \int_{S_{e\min}}^{1} dS_e/\psi^2} \quad (23)$$

Instead of presenting the MQ formula based on the CCG model in the form of finite sums, as is usually done in the literature, we believe that it is worthwhile to present the $K_r(S_e)$ relationship in terms of integrals for several reasons: (1) we can compare different formulae in an easier way, (2) if analytical relationships between ψ and S_e are available, the K-S_e relationship may also be obtained in a closed form, and (3) the computer permits use of a variety of procedures for replacing integrals by finite sums. This latter argument is of extreme importance, as will be shown later. For this reason, we have elaborated the CCG model (see Appendix 3) to obtain a final compact integral form of the K-θ relationship:

$$K_r(\theta) = S_e^{\alpha} \cdot \int_0^{\theta} (\theta - \vartheta)\, d\vartheta/\psi^2 \Big/ \int_0^{\theta_{sat}} (\theta_{sat} - \vartheta)\, d\vartheta/\psi^2 \quad (24)$$

Using $\alpha = 4/3$ and (15) to express the ψ-S_e dependence on the extrapolated portion, we have

$$K_r(S_e) = S_e^{4/3}\left[\frac{1}{\psi_{\min}^2}\left(\frac{S_e S_{e\min}}{1 + 2/\lambda} - \frac{S_{e\min}^2}{2 + 2/\lambda}\right) + \int_{S_{e\min}}^{S_e} (S_e - s)\, ds/\psi^2\right] \cdot \left[\frac{1}{\psi_{\min}^2}\left(\frac{S_{e\min}}{1 + 2/\lambda} - \frac{S_{e\min}^2}{2 + 2/\lambda}\right) + \int_{S_{e\min}}^{1} (1 - s)\, ds/\psi^2\right]^{-1} \quad (25)$$

which is the equivalent formula for the MQ model. Parameters ϑ and s (in (24) and (25)) are demivariables representing the effective water content and the effective saturation, respectively.

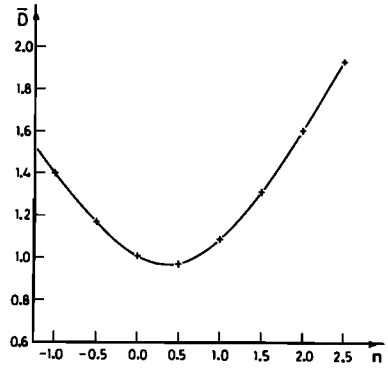

Fig. 2. Computed $\bar{D}$ based on 45 soils as a function of the power n (see (14)).

The numerical procedure used in this study is based on the assumption that the measured ψ-S_e curve can be very closely approximated by a continuous polygon, i. e., that ψ can be expressed by

$$\psi = \psi_i - \frac{(\psi_i - \psi_{i+1})}{(S_{ei+1} - S_{ei})}(S_e - S_{ei}) \quad (26)$$

$$S_{ei} \le S_e < S_{ei+1}$$

In this case we are not limited to using constant intervals, the node points are conveniently chosen with regard to the curvature of the given graph, and the computation of $K_r(S_e)$ is accurately performed. When (26) is used, (22) becomes

$$K_r(S_e) = S_e^{1/2}\left\{\left[S_{e\min}/(1 + 1/\lambda)\psi_{\min} + \sum_1^l \left(\frac{S_{ei+1} - S_{ei}}{\psi_i - \psi_{i+1}}\right) \ln\left(\frac{\psi_i}{\psi_{i+1}}\right)\right] \cdot \left[S_{e\min}/(1 + 1/\lambda)\psi_{\min} + \sum_1^m \left(\frac{S_{ei+1} - S_{ei}}{\psi_i - \psi_{i+1}}\right) \ln\left(\frac{\psi_i}{\psi_{i+1}}\right)\right]^{-1}\right\}^2 \quad (27)$$

while the WG and the modified MQ model ((23) and (25)) yield

$$K_r(S_e) = S_e^2\left\{\left[S_{e\min}/(1 + 2/\lambda)\psi_{\min}^2 + \sum_1^l \frac{S_{ei+1} - S_{ei}}{\psi_i \psi_{i+1}}\right]\left[S_{e\min}/(1 + 2/\lambda)\psi_{\min}^2 + \sum_1^m \frac{S_{ei+1} - S_{ei}}{\psi_i \psi_{i+1}}\right]\right\}^{-1} \quad (28)$$

and

$$K_r(S_e) = S_e^{4/3}\left\{\left[\frac{1}{\psi_{\min}^2}\left(\frac{S_e S_{e\min}}{1 + 2/\lambda} - \frac{S_{e\min}}{2 + 2/\lambda}\right)^2 + \sum_1^l \left[S_e \frac{S_{i+1} - S_i}{\psi_i \psi_{i+1}} - \left(\frac{S_{i+1} - S_i}{\psi_i - \psi_{i+1}}\right)\left(\frac{S_{i+1}}{\psi_{i+1}} - \frac{S_i}{\psi_i}\right) + \left(\frac{S_{i+1} - S_i}{\psi_i - \psi_{i+1}}\right)^2 \ln\left(\frac{\psi_i}{\psi_{i+1}}\right)\right]\right] \Big/ \left[\frac{1}{\psi_{\min}^2}\left(\frac{S_{e\min}}{1 + 2/\lambda} - \frac{S_{e\min}}{2 + 2/\lambda}\right)^2 + \sum_1^m \left[\frac{S_{i+1} - S_i}{\psi_i \psi_{i+1}} - \left(\frac{S_{i+1} - S_i}{\psi_i - \psi_{i+1}}\right) \cdot \left(\frac{S_{i+1}}{\psi_{i+1}} - \frac{S_i}{\psi_i}\right) + \left(\frac{S_{i+1} - S_i}{\psi_i - \psi_{i+1}}\right)^2 \ln\left(\frac{\psi_i}{\psi_{i+1}}\right)\right]\right]\right\} \quad (29)$$

respectively. In the following the suggested model ((27)), as well as the models of Averjanov, WG, and MQ ((1), (28), and (29), respectively), will be compared with the experimentally measured data.

In Table 3 the deviation D between the measured $K_r(S_e)$ curves and the computed ones (using the proposed method and the three methods mentioned above) is given for each one of the 45 soils. The italicized values indicate the model which yields the minimum deviation between the measured curves and the forecasted ones. The average value $\bar{D}$ for all 45 soils, the standard deviation σ, and the coefficient of variance ϵ are given in the last three lines of the table. It may be seen that for various soils, best results are achieved by different methods. This can also be concluded from Figures 3*a*–3*p*, in which the computed results are shown for a sample of 16 soils. On the other hand, comparison between the different models on an overall basis shows that best results are achieved by the proposed model. This is reflected by the number of soils for which D is minimum (see Table 3 and Figures 3*f*, 3*g*, 3*j*, and 3*m*–3*p*) and by the computed average value $\bar{D}$ for the 45 soils.

Very often the agreement of Averjanov's model with the experimental data is quite poor (as it is in soils 1006, 3302, 3305, 3306, 3403, 3404, 3405, and 3407; see also Figures 3*a* and 3*c*–3*f*), while in some cases (soils 2002, 4121, and 4126; see Figures 3*b* and 3*l*) a definite improvement in results is achieved by this method as compared with the other three. It seems, therefore, that the ψ-θ curve includes some inherent characteristic properties of the soil, which the generalized Kozeny-Averjanov-Irmay approach ignores. One may conclude, however, that Averjanov's model fits sands well, while it fails to describe the K_r-Θ relationship accurately for heavier soils. Yet the Averjanov-Irmay type of equation, with adjustable power, is an expression that has been proved to be very convenient in the analytical solution of partly saturated flow problems. It might be possible to improve prediction of $K(\Theta)$ by adjusting the power for tortuosity and for λ (as was done by *Brooks and Corey* [1964] or as shown here in (16)).

Among the other three models the WG model yields the poorest results. For soils in which $d\theta/d\psi \neq 0$ as $\psi \to 0$, there is an abrupt fall of the computed hydraulic conductivity near saturation (Figures 3*b*, 3*d*, 3*e*, 3*h*–3*l*, and 3*n*). For some soils these computed results are justified by the experimental data (Figure 3*e*), but in most cases the contrary is sustained, since the observed drop is milder.

Finally, we believe that there is a good chance of improving the prediction of $K_r(\Theta)$ by developing procedures which circumvent some of the existing limitations. One might neglect the measured data of ψ-Θ near saturation and fix a clear air entry value. Another modification is the derivation and use of an experimental correlation between the value of n in the power function ((1)) and some physical parameters of the soils.

SUMMARY AND CONCLUSIONS

The new model for prediction of $K_r(\Theta)$, proposed herein, is based on a reasonable approximate evaluation of the hydraulic conductivity of a pore domain with varying shape. The $K_r(\Theta)$ expression is derived in a simple integral form. Thus in cases where the ψ-Θ dependence is given by analytical formulae, $K_r(\Theta)$ can be reduced to a closed form. Very rarely is the ψ-Θ curve measured in the whole range. Hence in order to make the various models more practical tools an analytical procedure is suggested for the determination of the residual water content and the extrapolation of the ψ-Θ curve into the range for which no measured data are available.

The presentation of the CCG model is modified to derive a compact integral formula instead of its usual form in finite sum. This improvement enables us to use the same modified procedures in applying the various models and therefore to perform a more reliable comparison among the models.

For computational benefit the measured ψ-Θ curve is regarded as a continuous polygon connecting the given (ψ, Θ) points. This approximation ensures an accurate computation of $K_r(S_e)$ without truncation errors (which are quite significant for values of ψ near zero).

The proposed model, as well as the three main existing models of Averjanov, MQ, and WG, is compared with measured data of various soils. Since this test is carried out against data the accuracy of which is undetermined, 45 soils of different types are considered to ensure solid conclusions. It is

TABLE 3. Deviation D Between the Measured and Computed $K_r(S_e)$ Obtained by Using the Models of Averjanov, WG, and MQ and the Proposed Model

No.	Soil Index	D			
		Averjanov	WG	MQ	Proposed Model
1	1006	1.94	*0.20*	0.24	0.29
2	1101	1.26	0.74	0.76	*0.64*
3	2002	*1.72*	6.01	4.38	4.17
4	2004	0.22	*0.14*	0.19	0.40
5	3001	1.08	0.37	*0.23*	0.76
6	3002	0.51	0.36	*0.25*	0.46
7	3101	0.59	1.01	1.18	0.58
8	3301	*0.59*	2.44	1.48	1.22
9	3302	5.67	*1.07*	1.69	1.72
10	3304	0.63	0.49	0.58	*0.42*
11	3305	5.12	*1.13*	1.28	1.34
12	3306	6.11	2.36	*1.26*	1.34
13	3307	0.46	*0.33*	0.44	0.38
14	3403	4.38	1.38	1.15	*0.94*
15	3404	4.87	2.82	1.59	*1.33*
16	3405	5.46	*1.00*	2.23	2.18
17	3407	1.96	0.82	0.44	*0.25*
18	3501	0.42	0.86	1.04	*0.40*
19	3503	2.18	4.33	*2.01*	2.25
20	3504	2.66	2.93	*1.61*	1.67
21	4106	*0.50*	1.00	1.03	0.65
22	4107	0.38	0.62	0.71	*0.30*
23	4109	1.12	0.88	1.18	*0.56*
24	4111	1.13	2.03	1.82	*1.01*
25	4114	1.18	0.92	*0.59*	0.77
26	4116	0.55	*0.54*	0.60	0.97
27	4118	*0.52*	1.19	1.73	0.86
28	4120	*0.66*	0.80	1.02	0.79
29	4121	*0.27*	3.53	2.77	2.41
30	4123	0.80	0.70	*0.53*	0.97
31	4126	*0.28*	2.15	1.21	1.22
32	4129	*0.88*	2.65	2.65	2.26
33	4130	*0.14*	0.24	0.26	0.27
34	4131	0.56	0.43	*0.34*	0.62
35	4132	*2.85*	3.53	3.66	2.91
36	4133	0.37	0.41	*0.36*	0.44
37	4134	0.31	0.35	0.56	*0.30*
38	4137	0.53	0.28	0.53	*0.16*
39	4141	1.38	1.60	1.71	*0.93*
40	4142	0.65	0.99	0.62	0.91
41	4143	0.52	0.73	0.92	*0.41*
42	4147	0.71	0.50	0.70	*0.37*
43	5002	0.91	0.98	1.12	*0.43*
44	5003	0.61	0.69	1.04	*0.21*
45	5004	0.90	0.80	1.04	*0.30*
$\bar{D}$		1.49	1.32	1.17	*0.97*
σ		1.64	1.22	0.88	0.82
$\epsilon = \sigma/D$		1.10	0.93	0.75	0.84

The italicized values indicate the model which yields the minimum deviation between the measured curves and the forecasted ones.

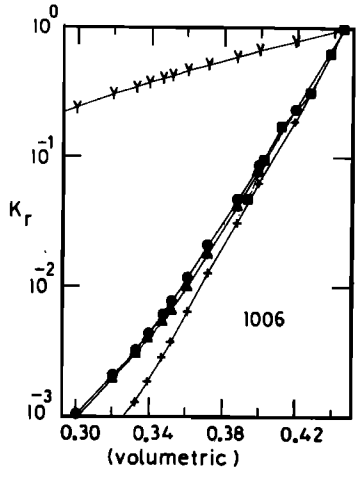

Fig. 3*a*

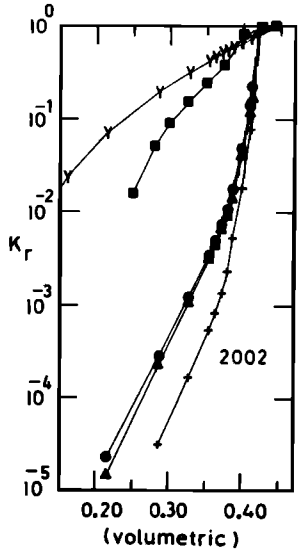

Fig. 3*b*

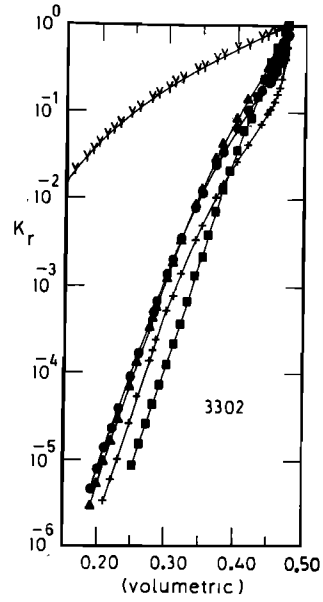

Fig. 3*c*

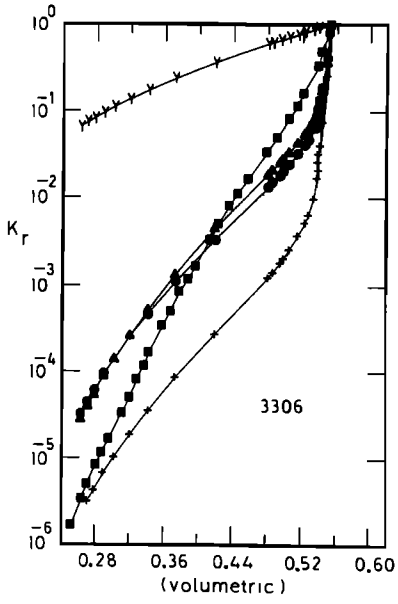

Fig. 3*d*

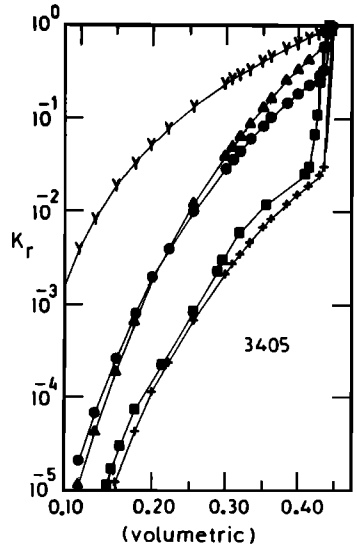

Fig. 3*e*

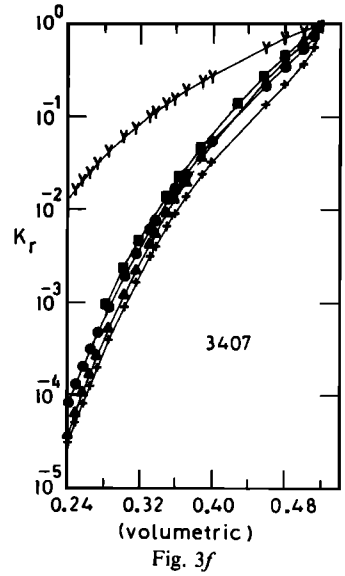

Fig. 3*f*

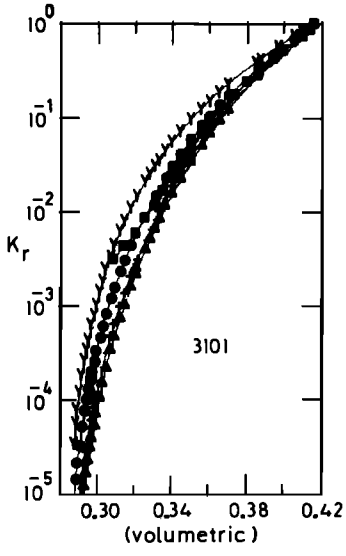

Fig. 3*g*

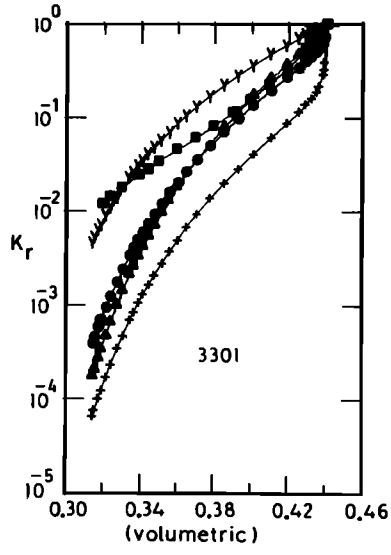

Fig. 3*h*

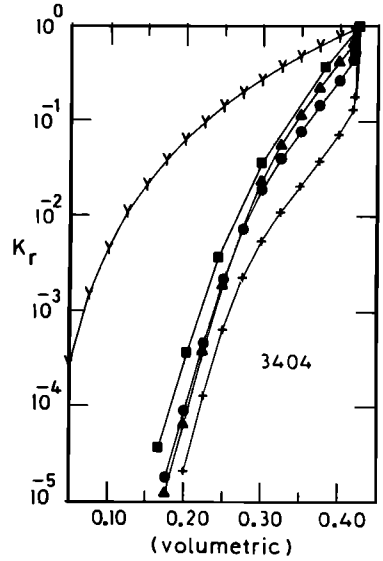

Fig. 3*i*

Fig. 3. Computed relative hydraulic conductivities for 16 soils using four models: Averjanov's (Y symbols; see (1)), WG's (plusses; see (28)), MQ's (solid triangles; see (29)), and the proposed model (solid circles; see (27)). The measured curve is shown by solid squares.

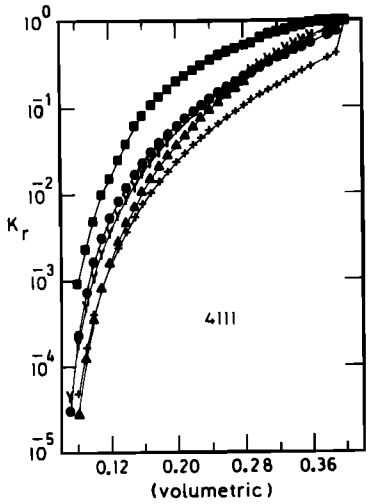

Fig. 3*j*

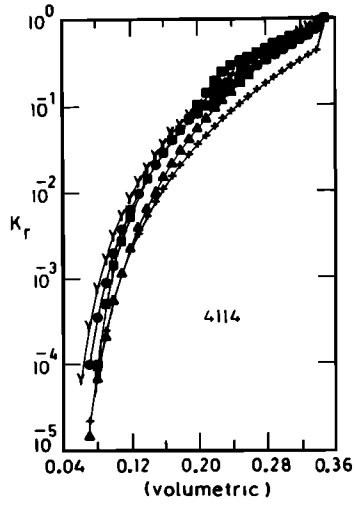

Fig. 3*k*

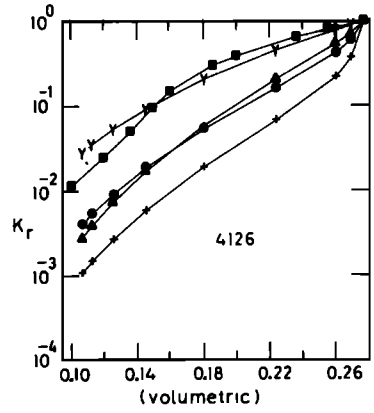

Fig. 3*l*

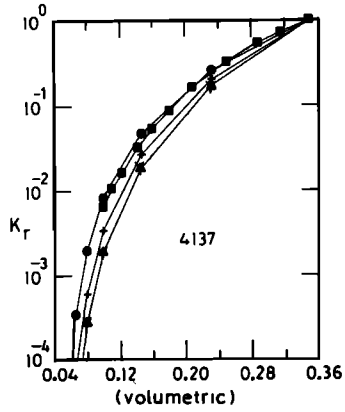

Fig. 3*m*

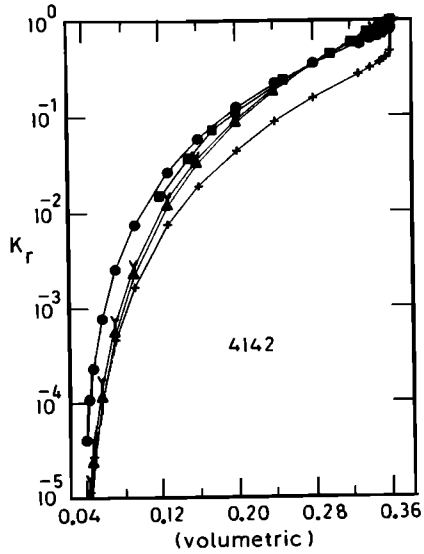

Fig. 3*n*

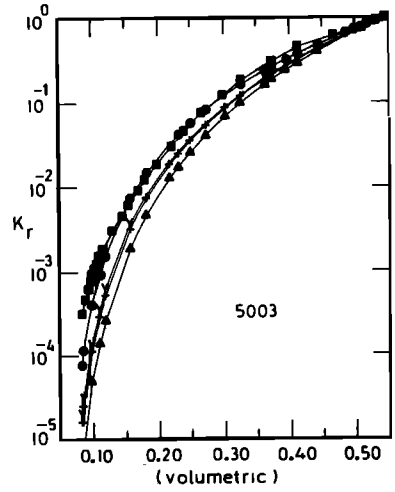

Fig. 3*o*

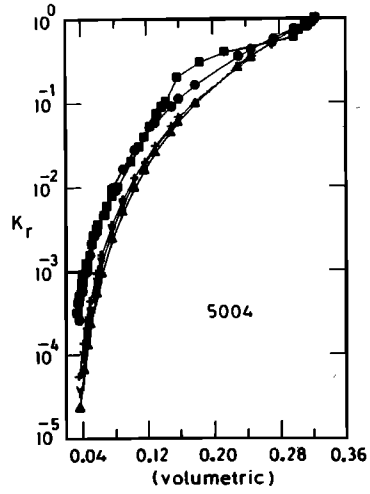

Fig. 3*p*

Fig. 3. (continued)

shown that the proposed model is more reliable than the existing models and clearly improves the prediction of unsaturated hydraulic conductivities.

APPENDIX 1: HYDRAULIC CONDUCTIVITY OF THE CAPILLARY ELEMENT

In most of the rational models for predicting K one considers the conductivity of a pair (or a series) of capillary elements. Relying on Poiseuille's equation, *Childs and Collis-George* [1950] assumed that the conductivity is determined by the radius of the narrower element, whereas *Wyllie and Gardner* [1958] used a reduced pore radius. Here a different relationship is adopted, based on the pore configuration shown in Figure 1.

To simplify matters, we disregard special effects and assume that each capillary in Figure 1 obeys the Poiseuille equation, i.e.,

$$Q_1 = -\frac{\pi r^4 g}{8\nu}\frac{d\phi}{dx} \qquad Q_2 = -\frac{\pi r^4 g}{8\nu}\frac{d\phi}{dx} \tag{A1}$$

where $\phi = \psi + z$ is the head, ν is the liquid kinematic viscosity, and Q is the discharge. For this combination in series, the total head loss is

$$\Delta\phi = \Delta\phi_1 + \Delta\phi_2 \tag{A2}$$

while the discharge is

$$Q = Q_1 = Q_2 \tag{A3}$$

If the element of Figure 1 is replaced by an equivalent tube of radius R and length L, then the discharge relationship yields

$$R^4\,\Delta\phi/L = r^4\,\Delta\phi_1/l_1 = \rho^4\,\Delta\phi_2/l_2 \tag{A4}$$

while equivalency of volumes gives

$$R^2L = r^2l_1 + \rho^2l_2 \tag{A5}$$

Assuming moreover that the lengths are proportional to the radii [*Fatt*, 1956],

$$l_1/l_2 = r/\rho \tag{A6}$$

we obtain

$$R^2 = r\rho \tag{A7}$$

This means that the 'large pore' has a more important influence than is generally assumed. The reason is, of course, that we have taken into account its length and not only its cross section.

APPENDIX 2: PROCEDURE FOR DETERMINATION OF Θ_r AND THE EXTRAPOLATED ψ-Θ CURVE

The determination of Θ_r is a prerequisite for using any of the methods suggested for predicting the K-Θ relationship. We define Θ_r as the residual water content for $d\Theta/d\psi \to 0$ for $\Theta \to \Theta_r$ because it fulfils the other basic requirement that $K(\Theta_r) = 0$. Very often, only part of the ψ-Θ curve is measured, Θ_r is an unknown parameter, and it is not clear how to extrapolate the measured curve. This problem becomes embarrassing when comparisons of various models with measurements are studied, because just by choosing Θ_r we may improve or worsen one method in relation to the others. There is an intense need for an objective analytic procedure for extrapolating the measured ψ-Θ curve.

In this work, (15) is adopted to represent the extrapolated part of the ψ-Θ curve. Demanding that the extrapolated curve should pass through the measured last point ($\psi_{\min}$, $\Theta_{\min}$) leads to

$$\frac{S_e}{S_{e\,\min}} = \frac{\Theta - \Theta_r}{\Theta_{\min} - \Theta_r} = \left(\frac{\psi_{\min}}{\psi}\right)^{\lambda} \tag{A8}$$

or

$$\ln(\psi_{\min}/\psi) = \lambda^{-1}\ln(S_e/S_{e\,\min}) \tag{A9}$$

On a log scale, (9) describes a straight line. As a matter of convenience we define

$$y = \ln(\psi_{\min}/\psi) \qquad x = \ln(S/S_{\min}) \tag{A10}$$

Since the extrapolated curve should match the measured one, we demand that the dispersion of the measured points, up to the inflection Θ_p point ($\Theta_{\min} < \Theta < \Theta_p$), around the analytic curve (A9) should be minimum. The sum of the square deviation of the measured data from the analytic curve is

$$d = \sum_1^N [y_i - y(x_i)]^2 = \sum_1^N \left(y_i^2 - \frac{2}{\lambda}y_ix_i + \frac{1}{\lambda^2}x_i^2\right) \tag{A11}$$

and requiring d to be minimum ($\partial d/\partial\lambda = 0$), one obtains

$$\lambda = \sum_1^N \left[\ln\left(\frac{S_i}{S_{\min}}\right)\right]^2 \Big/ \sum_1^N \ln\left(\frac{\psi_{\min}}{\psi_i}\right)\ln\left(\frac{S_i}{S_{\min}}\right) \tag{A12}$$

and

$$d = \sum_1^N \left[\ln\left(\frac{\psi_{\min}}{\psi_i}\right)\right]^2 - \frac{2}{\lambda}\sum_1^N \ln\left(\frac{\psi_{\min}}{\psi_i}\right)\ln\left(\frac{S_i}{S_{\min}}\right) + \frac{1}{\lambda^2}\sum_1^N \left[\ln\left(\frac{S_i}{S_{\min}}\right)\right] \tag{A13}$$

If we assume a series value $\Theta_{rj} = 0.01j$, $j = 1, 2, \cdots$, up to $\Theta_{\min}$, the corresponding λ_j and d_j are obtained by using (A12) and (A13). The residual water content Θ_r is chosen as the value of Θ_{rj} which yields the minimum value of d_j.

APPENDIX 3: MODIFIED FORMULATION OF THE CCG MODEL

The basic equation suggested by *Childs and Collis-George* [1950] as set forth by *Brutsaert* [1967] is

$$K(R) = M\int_{\rho=R_{\min}}^{\rho=R}\int_{r=R_{\min}}^{r=\rho} r^2f(\rho)f(r)\,dr\,d\rho + M\int_{\rho=R_{\min}}^{\rho=R}\int_{r=\rho}^{r=R} \rho^2f(r)f(\rho)\,d\rho\,dr \tag{A14}$$

It is obvious that the integration is carried over the square domain OABC in the (r, ρ) plane (Figure 4). The first integral (left-hand side) of (A14) is carried over the triangle OBC, and the second integral over the complementary triangle OAB. By a change in the order of integration,

$$\int_{\rho=R_{\min}}^{\rho=R}\int_{r=R_{\min}}^{r=\rho} r^2f(\rho)f(r)\,dr\,d\rho = \int_{r=R_{\min}}^{r=R}\int_{\rho=r}^{\rho=R} r^2f(r)f(\rho)\,d\rho\,dr \tag{A15}$$

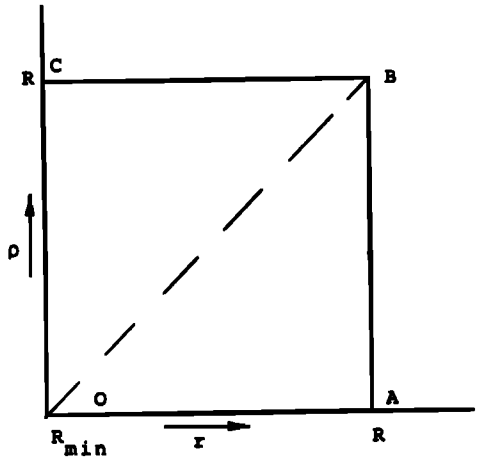

Fig. 4. Description of the integration domain of (A14).

and a change of variables,

$$\int_{r=R_{\min}}^{r=R}\int_{\rho=r}^{\rho=R} r^2 f(r)f(\rho)\,d\rho\,dr = \int_{\rho=R_{\min}}^{\rho=R}\int_{r=\rho}^{r=R} \rho^2 f(\rho)f(r)\,dr\,d\rho \qquad \text{(A16)}$$

it follows that the two integrals of (A14) are identical. Hence

$$K(R) = 2M\int_{\rho=R_{\min}}^{\rho=R}\int_{r=\rho}^{r=R} \rho^2 f(\rho)f(r)\,dr\,d\rho = 2M\int_{\rho=R_{\min}}^{\rho=R} \rho^2 f(\rho)\int_{r=\rho}^{r=R} f(r)\,dr\,d\rho \qquad \text{(A17)}$$

By definition, we have

$$\int_{R_{\min}}^{R} f(r)\,dr = \theta(R) \qquad \text{(A18)}$$

and substituting in (A17) we obtain

$$K(\theta) = 2M'\int_0^{\theta}(\theta - \vartheta)\frac{1}{\psi^2}\,d\vartheta \qquad \text{(A19)}$$

By matching at saturation, the CCG formula can be written as

$$K_r(\theta) = \int_0^{\theta}(\theta - \vartheta)\frac{d\vartheta}{\psi^2}\Big/\int_0^{\theta_{sat}}(\theta_{sat} - \vartheta)\frac{d\vartheta}{\psi^2} \qquad \text{(A20)}$$

The formulae of *Millington and Quirk* [1961] and *Kunze et al.* [1968] may be written similarly by multiplying the right-hand side of (A19) by S_e^n, with $n = \frac{1}{3}$ and $n = 1$, respectively.

NOTATION

- a probability.
- $f(r)$ pore water distribution function.
- G correlation factor.
- K hydraulic conductivity.
- K_r, K_{rc} relative hydraulic conductivity and computed value of K_r.
- l index.
- L, l length.
- m index.
- n constant power.
- R, r radius.
- $S_e, S_{e\,\min}$ effective saturation and minimum effective saturation.
- T tortuosity factor.
- α, β constant power.
- Θ, Θ_r actual and residual water content.
- $\Theta_{max}, \Theta_{min}$ measured maximum and minimum values of Θ.
- $\theta = \Theta - \Theta_r$, effective water content.
- ρ radius.
- ψ capillary head.
- ψ_{cr} capillary head at which $d\theta/d\psi > 0$.
- ψ_{min} minimum measured value of ψ.

Acknowledgment. The present work has been supported by the U.S.-Israel Science Binational Foundation under grant 442.

REFERENCES

Averjanov, S. F., About permeability of subsurface soils in case of incomplete saturation, *Eng. Collect., 7,* 1950.

Black, T. A., W. R. Gardner, and G. W. Thirtell, The prediction of evaporation, drainage, and soil water storage for a bare soil, *Soil Sci. Soc. Amer. Proc., 33,* 655–660, 1969.

Boreli, M., and G. Vachaud, Note sur la determination de la teneur en eau résiduelle et sur la variation de la perméabilité relative dans les sols non saturés, *C. R. Acad. Sci., 263,* 698–701, 1966.

Brooks, R. H., and A. T. Corey, Hydraulic properties of porous media, *Hydrol. Pap. 3,* Colo. State Univ., Fort Collins, 1964.

Brooks, R. H., and A. T. Corey, Properties of porous media affecting fluid flow, *J. Irrig. Drain. Div. Amer. Soc. Civil Eng., 92*(IR2), 61–88, 1966.

Bruce, R. R., Hydraulic conductivity evaluation of the soil profile from soil water retention relations, *Soil Sci. Soc. Amer. Proc., 36,* 555–560, 1972.

Brutsaert, W., Some methods of calculating unsaturated permeability, *Trans. ASAE, 10,* 400–404, 1967.

Burdine, N. T., Relative permeability calculation from size distribution data, *Trans. AIME, 198,* 71–78, 1953.

Childs, E. C., and N. Collis-George, The permeability of porous materials, *Proc. Roy. Soc., Ser. A, 201,* 392–405, 1950.

Elrick, D. E., and D. H. Bowman, Note on an improved apparatus for soil moisture measurements, *Soil Sci. Soc. Amer. Proc., 28,* 450–453, 1964.

Farrell, D. A., and W. E. Larson, Modeling the pore structure of porous media, *Water Resour. Res., 8,* 699–706, 1972.

Fatt, I., The network model of porous media, 1, 2, 3, *Trans. AIME, 207,* 144–181, 1956.

Gardner, W. R., Mathematics of isothermal water conduction in unsaturated soils, *Rep. 40,* pp. 78–87, Highway Res. Board, Nat. Res. Counc., Washington, D. C., 1959.

Green, R. E., and J. C. Corey, Calculation of hydraulic conductivity: A further evaluation of some predictive methods, *Soil Sci. Soc. Amer. Proc., 35,* 3–8, 1971.

Green, R. E., R. J. Hanks, and W. E. Larson, Estimates of field infiltration by numerical solution of the moisture flow equation, *Soil Sci. Soc. Amer. Proc., 28,* 15–19, 1964.

Hadas, A., Evaporation and drying process in layered soils (in Hebrew), Ph.D. thesis, Hebrew Univ., Rehovot, Israel, 1967.

Irmay, S., On the hydraulic conductivity of unsaturated soils, *Eos Trans. AGU, 35,* 463–467, 1954.

Jackson, R. D., R. J. Reginato, and C. H. M. Van Bavel, Comparison of measured and calculated hydraulic conductivities of unsaturated soils, *Water Resour. Res., 1*(3), 375–380, 1965.

Jensen, M. E., and R. J. Hanks, Nonsteady state drainage from porous media, *J. Irrig. Drain. Div. Amer. Soc. Civil Eng., 93*(IR3), 209–231, 1967.

Kastelanek, F., Numerical simulation technique for vertical drainage, *J. Hydrol., 14,* 213–232, 1971.

Kunze, R. J., G. Uehara, and K. Graham, Factors important in the calculation of hydraulic conductivity, *Soil Sci. Soc. Amer. Proc., 32,* 760–765, 1968.

Marshall, T. J., A relation between permeability and size distribution of pores, *J. Soil Sci., 9,* 1–8, 1958.

Millington, R. J., and J. P. Quirk, Permeability of porous solids, *Trans. Faraday Soc., 57,* 1200–1206, 1961.

Nielsen, D. R., D. Kirkham, and E. R. Perrier, Soil capillary conductivity: Comparison of measured and calculated values, *Soil Sci. Soc. Amer. Proc., 24,* 157–160, 1960.

Poulovassilis, A., Hysteresis of pore water in granular porous bodies, *Soil Sci., 109,* 5–12, 1970.

Rawitz, E., The influence of a number of environmental factors on the availability of soil moisture to plants (in Hebrew), Ph.D. thesis, Hebrew Univ., Rehovot, Israel, 1965.

Staple, W. J., Moisture tension, diffusivity and drying, *Can. J. Soil Sci., 45,* 78–85, 1965.

Talsma, T., Hysteresis in two sands and the independent domain model, *Water Resour. Res., 6*(3), 964–970, 1970.

Topp, G. C., Soil water hysteresis measured in a sandy loam compared with the hysteretic domain model, *Soil Sci. Soc. Amer. Proc., 33,* 645–651, 1969.

Topp, G. C., Soil water hysteresis in silt loam and clay loam soils, *Water Resour. Res., 7*(4), 914–920, 1971.

Topp, G. C., and E. E. Miller, Hysteresis moisture characteristics and hydraulic conductivities for glass-bead media, *Soil Sci. Soc. Amer. Proc., 30,* 156–162, 1966.

Vachaud, G., Vérification de la loi de Darcy generalisée et détermination de la conductivité capillaire partir d'une infiltration horizontal, *Ass. Int. Hydrol. Sci. Wageningen, 82,* 277–292, 1966.

Watson, K. K., Experimental and numerical study of column drainage, *J. Hydraul. Div. Amer. Soc. Civil Eng., 93,* 1–15, 1967.

Wyllie, M. R. J., and G. H. F. Gardner, The generalized Kozeney-Carman equation, *World Oil, 146,* 210–228, 1958.

(Received February 21, 1975;
revised August 11, 1975;
accepted August 15, 1975.)